PALAIOS
Emphasizing the impact of life on Earth's history

PALAIOS, 2009, v. 24, p. 318–328
Research Article
DOI: 10.2110/palo.2008.p08-057r

THE PALEOCENE–EOCENE THERMAL MAXIMUM: NEW DATA ON MICROFOSSIL TURNOVER AT THE ZUMAIA SECTION, SPAIN

LAIA ALEGRET,[1]* SILVIA ORTIZ,[1,2] XABIER ORUE-ETXEBARRIA,[3] GILEN BERNAOLA,[3,4] JUAN I. BACETA,[3] SIMONETTA MONECHI,[5] ESTIBALIZ APELLANIZ,[3] and VICTORIANO PUJALTE[3]

[1]*Universidad de Zaragoza, Departamento de Ciencias de la Tierra, Facultad de Ciencias, 50009 Zaragoza, Spain;* [2]*University College London, Department of Earth Sciences, WC1E 6BT London, UK;* [3]*Universidad del País Vasco, Departamento de Estratigrafía y Paleontología, Facultad de Ciencia y Tecnología, 48080 Bilbao, Spain;* [4]*Universidad del País Vasco, Departamento de Ingeniería Minera y Metalúrgica y CC de los Materiales, Escuela Universitaria de Ingeniería Técnica de Minas y de Obras Públicas, 48901 Barakaldo, Spain;* [5]*Università degli Studi di Firenze, Dipàrtimento di Scienze della Terra, Via La Pira, 4, 50121 Florence, Italy*

e-mail: laia@unizar.es

ABSTRACT

The benthic foraminiferal turnover and extinction event (BEE) associated with the negative carbon isotope excursion (CIE) across the Paleocene–Eocene Thermal Maximum (PETM) is analyzed in the Zumaia section (Spain), one of the most complete and expanded deep-water sequences known worldwide. New biostratigraphic, paleoecologic, and paleoenvironmental data on benthic foraminifera are correlated to information on planktic foraminiferal and calcareous nannofossil turnover in order to evaluate possible causes and consequences of the PETM. Gradual but rapid extinction of 18% of the benthic foraminiferal species starts at the onset of the CIE, after the initial ocean warming (as inferred from calcareous nannofossils) recorded in the last 46 kyr of the Paleocene. This gradual extinction event culminated ~10.5 kyr after the onset of the CIE and led to the main BEE, affecting 37% of the species. Therefore, extinctions across the PETM affected a total of 55% of the benthic foraminiferal species at Zumaia. The gradual extinction occurred under inferred oxic conditions without evidence for carbonate dissolution, indicating that carbonate corrosivity and oxygenation of the ocean bottom waters were not the main cause of the event. An interval characterized by dissolution occurs above the main BEE, suggesting that bottom waters became corrosive after the main extinction. Carbonate is progressively better preserved through the overlying deposits, and carbon isotope values gradually return to background levels. These data are consistent with a slow deepening of the carbonate compensation depth after its initial rise owing to abrupt acidification of the oceans. Microfossil data support a rapid onset of the PETM, followed by long-term effects on calcareous plankton and benthic foraminifera.

INTRODUCTION

A major, rapid extinction of deep-sea benthic foraminifera occurred at the Paleocene-Eocene (PE) boundary (e.g., Tjalsma and Lohmann, 1983; Thomas, 1989), ~55 Ma. The extinction was coeval with an episode of extreme global warming called the Paleocene–Eocene Thermal Maximum (PETM), during which temperatures increased up to 9°–10°C in high-latitude, surface waters and up to ~5°C in the deep sea, in equatorial surface waters, and on land at midlatitudes in continental interiors (see references in Thomas, 2007).

A negative 2.5‰–6‰ carbon isotope excursion (CIE) in marine and terrestrial $\delta^{13}C$ values of carbonate and organic carbon is associated with the PETM (e.g., Kennett and Stott, 1991; Thomas and Shackleton, 1996; Zachos et al., 2001; Bowen et al., 2006; Sluijs et al., 2007a), and its onset formally marks the base of the Eocene (Aubry et al., 2007). This excursion reflects a major perturbation in the global carbon cycle, which affected the whole ocean-atmosphere system. The Calcite Compensation Depth (CCD) rose by >2 km in the South Atlantic Ocean (Zachos et al., 2005), which has been interpreted in terms of a rapid input of isotopically light carbon into the ocean-atmosphere system, perhaps by the massive dissociation of marine methane hydrates caused by processes such as continental slope failure, a drop in sea level, the impact of an extraterrestrial body, or volcanism (for an overview, see Thomas, 2007). Actual shoaling documented in Ocean Drilling Program (ODP) drilling, however, was substantially larger than can be explained by methane dissociation alone (Zachos et al., 2005; Thomas, 2007). The onset of these anomalies occurred during a time period of <20 kyr (Kennett and Stott, 1991; Katz et al., 1999; Röhl et al., 2000, 2007), whereas the return to more normal values occurred over longer time scales of 10^5 years (Dickens et al., 1995; Katz et al., 1999; Röhl et al., 2007; Sluijs et al., 2007a; Westerhold et al., 2007).

The PETM may not have been a singular event; rather, it may have been only the most severe out of a series of global warming events (e.g., the mid-Paleocene biotic event, the early Eocene ELMO—the Eocene layer of mysterious origin at Walvis Ridge—and X warming events) that are coupled with carbon isotope anomalies and carbonate dissolution (Thomas et al., 2000; Lourens et al., 2005; Bernaola et al., 2007). If the PETM was one of a series of events occurring at orbital periodicities (Lourens et al., 2005), its cause probably was not singular (e.g., a comet impact or a volcanic eruption) but intrinsic to Earth's climate system (Thomas, 2007).

Whatever the triggering mechanism, and whether or not the CIE was the result of dissociation of gas hydrates or other causes (see references in Thomas, 2007), the onset of the PETM was characterized by abrupt changes, such as the acidification of the oceans, and rapid changes in terrestrial and marine biota, including the largest extinction of benthic foraminifera (30%–50% of the species) recorded during the Cenozoic. Other major biological changes include a rapid evolutionary turnover of planktic foraminifera (e.g., Arenillas and Molina, 1996; Kelly et al., 1998) and calcareous nannoplankton (Aubry, 1995; Bralower, 2002; Stoll, 2005), the global acme of the dinoflagellate genus *Apectodinium* and its migration to high latitudes (Crouch et al., 2001; Sluijs et al., 2007a, 2007b), the rapid diversification of shallow-water larger benthic foraminifera (Orue-Etxebarria et al., 2001; Pujalte et al., 2003), latitudinal migration of plants (Wing et al., 2005), and a rapid radiation of mammals on land (e.g., Koch et al., 1992). The linkages between carbon cycle perturbation and coeval biotic changes are not completely understood. Individual ecosystems may have responded directly to such aspects of environmental change as carbon addition (ocean acidification, elevated pCO_2) or indirectly to consequences of carbon release, such as rising

* Corresponding author.

 0883-1351/09/0024-0318/$3.00

temperatures, increased precipitation, and changes in nutrient supply or distribution, and so forth (Bowen et al., 2006).

The benthic foraminiferal extinction event (BEE) lasted <10 kyr (Thomas, 2007), and its cause is not yet clear. The study of the BEE is interesting because deep-sea benthic foraminifera had survived without significant extinction through global environmental crises like those related to the asteroid impact at the end of the Cretaceous (e.g. Thomas, 1990; Alegret and Thomas, 2005; Alegret, 2007). While deep-sea benthic foraminifera suffered major extinction across the PETM, benthic foraminifera from marginal and epicontinental basins show less extinction or temporary assemblage changes. In shallow settings, increased biological productivity and anoxia at the seafloor have been documented across the PETM (e.g., Speijer and Wagner, 2002; Gavrilov et al., 2003; Alegret et al., 2005; Alegret and Ortiz, 2006). Increased runoff or upwelling currents could have led to high productivity and eutrophication, which, combined with low-oxygen concentrations, resulted in high total organic carbon in sediments from proximal settings (Tremolada and Bralower, 2004). Data from open ocean sites do not support global hypoxia, however, and are inconsistent with regard to global productivity changes (e.g., Gibbs et al., 2006; Thomas, 2007).

Several causes for triggering the BEE have been suggested (see Thomas, 2007, for a review), including (1) low oxygenation, either as a result of increased deep-sea temperatures or as a result of oxidation of methane in the water column; (2) increased corrosivity of the waters for $CaCO_3$ as a result of methane oxidation or incursion of CO_2 from the atmosphere; (3) increased or decreased productivity or expansion of the trophic resource continuum; or (4) a combination of several of these. The ultimate cause of the BEE, however, is not yet clear; climatic warming is the only common factor recorded worldwide. High temperatures would increase metabolic rates, and even under stable productivity in the oceans, organisms would indicate oligotrophic conditions because of their higher metabolic rates (Thomas, 2003, 2007).

More detailed analyses of benthic foraminifera across the PETM are thus needed in order to look into the causes of the BEE and of the benthic foraminiferal turnover. The Zumaia section (Western Pyrenees) contains one of the most complete and expanded deep-water successions across the Paleocene–Eocene transition yet reported (e.g., Molina et al., 1999; Baceta et al., 2000). This section has no recognizable biostratigraphic gaps or condensation, shows a high-sedimentation rate, identifiable geochemical and geomagnetic signals (minor diagenetic alteration), and abundant, well-diversified, open marine microfossils such as benthic and planktic foraminifera and calcareous nannofossils (Orue-Etxebarria et al., 2004). Different cyclostratigraphic, micropaleontologic, magnetostratigraphic, and chemostratigraphic studies have been completed based on this section (e.g., Canudo et al., 1995; Schmitz et al., 1997; Arenillas and Molina, 2000; Baceta et al., 2000; Dinarès-Turell et al., 2002; Orue-Etxebarria et al., 2004; Angori et al., 2007), but publications dealing with Paleocene–Eocene benthic foraminifera from Zumaia are scarce. Ortiz (1995) described assemblages from the upper Paleocene and lower Eocene, analyzing only a few samples from the lowermost Eocene. Kuhnt and Kaminski (1997) compiled data on agglutinated foraminifera from the latter publication, whereas Schmitz et al. (1997) pointed out the biostratigraphic distribution of some calcareous benthic foraminiferal taxa across the BEE. Here we present a new, high-resolution biostratigraphic, paleoecologic, and paleoenvironmental study of agglutinated and calcareous benthic foraminiferal assemblages and correlate data on benthic foraminifera to published data on the planktic foraminifera and calcareous nannofossils (Orue-Etxebarria et al., 2004; Angori et al., 2007).

GEOLOGIC SETTING AND METHODS

The Zumaia section (43°17.97′N, 2°15.65′W; see Fig. 1) is one of the most representative and complete outcrops of the (hemi)pelagic successions deposited in the Pyrenean basin during the Late Cretaceous–early

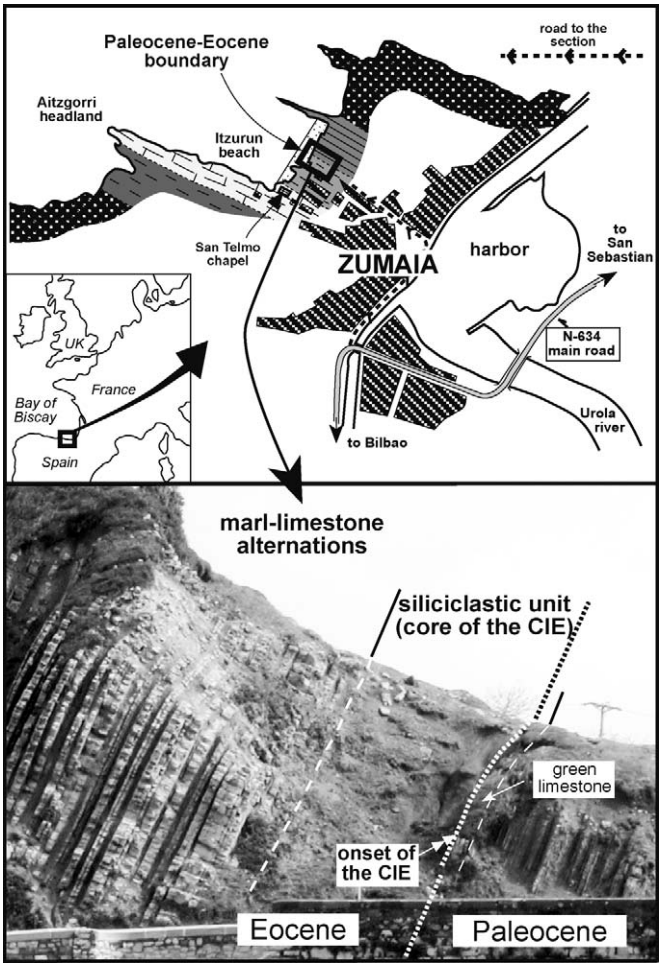

FIGURE 1—Location of the Paleocene–Eocene section in Zumaia, Spain. CIE = carbon isotope excursion marking Paleocene–Eocene boundary.

Paleogene (Baceta, 1996; Pujalte et al., 1998). The studied interval encompasses the uppermost 3 m of the Paleocene (Itzurun Formation; see Baceta et al., 2004) and the lowermost 7 m of the Eocene (Eocene Flysch); samples are spaced at 5–10 cm intervals in the lowermost 60 cm of the Eocene and at 0.1–1 m intervals below and above it (Fig. 2).

The lowermost 2 m of the studied section consists of alternations of marlstones and marly limestones, with intercalations of thin-bedded siliciclastic and mixed carbonate-siliciclastic turbidites. The uppermost 80 cm of the Paleocene (Itzurun Formation) consists of a distinct, hemipelagic limestone unit, called the green limestone, that includes a 4-cm-thick carbonate turbidite bed. The characteristic light green color of this limestone interval mainly results from the presence of glauconite, which occurs infilling many of the planktic and benthic foraminiferal tests (Baceta, 1996; Pujalte et al., 1998; Schmitz et al., 2000). Glauconite becomes more abundant toward the topmost 10 cm of the Paleocene (Schmitz et al., 1997), and it has also been observed at lower proportions in many hemipelagic limestones across the whole upper Paleocene of the Zumaia section (Baceta, 1996; Gawenda et al., 1999). In modern open-marine environments, authigenic glauconite may form at a wide range of depths (between 50 m and 1000 m) and is attributed to relatively low sedimentation rates (O'Brien et al., 1990; Balsam and Beeson, 2003).

The onset of the CIE occurs at the transition from the green limestone to the 35-cm-thick overlying marlstone interval (Schmitz et al., 1997), which records a progressive but rapid decrease in carbonate content. This marlstone is in turn overlain by a 4-m-thick interval made up mostly of carbonate-poor, reddish claystones and marls known as the siliciclastic unit (SU; see Schmitz et al., 2000; Fig. 2). The lower 1.7 m of the SU

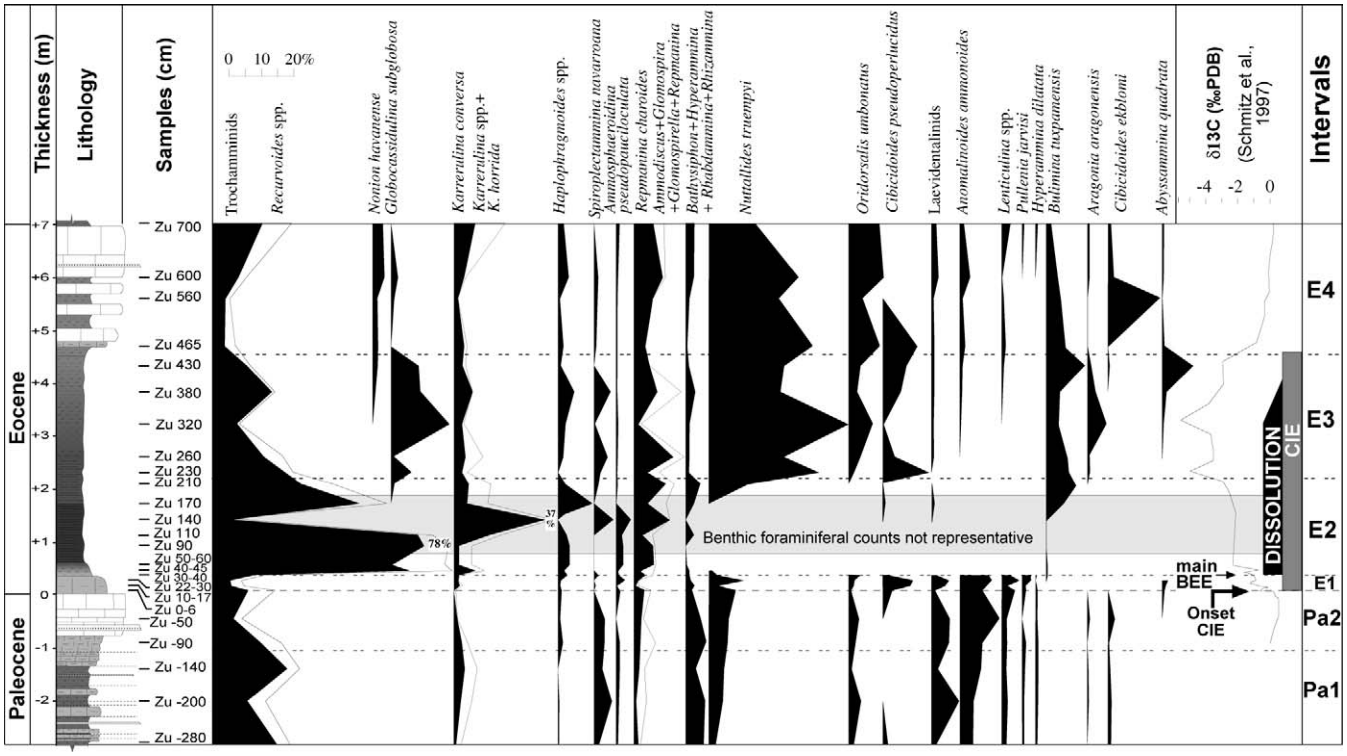

FIGURE 2—Stratigraphic distribution and relative abundance of benthic foraminiferal taxa across the upper Paleocene and lower Eocene at Zumaia and correlation to the $\delta^{13}C$ curve (in bulk sediment). Only taxa whose abundance is >2% in at least one sample have been plotted. BEE = benthic foraminiferal extinction event; CIE = carbon isotope excursion; PDB = Pee Dee Belemnite standard. Species that disappear in the lowermost Eocene (interval E1) are represented in Figure 3.

is almost devoid of carbonate and microfossils with calcareous tests, but these increase progressively in the upper 3.3 m (Schmitz et al., 1997; Orue-Etxebarria et al., 2004). Calcareous tests from this unit are very badly preserved and are partially dissolved; preservation of calcareous tests improves, and the planktic-benthic ratio increases, toward the upper part of the SU (samples Zu 380, Zu 430). The succession above is composed of alternating limestones and marls, the transition between them being gradual but rapid (Baceta et al., 2000).

Most of the studied material corresponds to the set of samples used by Orue-Etxebarria et al. (2004) for a study of planktic foraminifera and calcareous nannofossils. Some extra samples were collected in order to improve the sample resolution within the siliciclastic unit. Although turbidites are common at Zumaia, they are easily recognizable, and only *in situ* sediments were sampled. A total of 25 samples were analyzed for the benthic foraminiferal studies. Species richness calculations and quantitative studies of benthic foraminifera were based on representative splits (using a modified Otto microsplitter) of ~300 specimens >100 μm. All representative specimens were mounted on microslides for identification and a permanent record. Benthic foraminiferal counts are included in Supplementary Data[1]. Relative abundances of taxa (Figs. 2–3), the calcareous-agglutinated ratio, and several proxies for diversity, such as the Fisher α index and the H (S) Shannon-Weaver information function (Murray, 1991), were calculated (Fig. 4). Probable microhabitat preferences and environmental parameters were inferred from the benthic foraminiferal morphotype analysis (e.g., Bernhard, 1986; Jorissen et al., 1995; Kaminski and Gradstein, 2005) and from changes in diversity and in the relative abundance of selected taxa.

Paleodepth inferences were based on benthic foraminiferal data, mainly through comparison between fossil and recent assemblages, the occurrence and abundance of depth-related species, and their upper depth limits (e.g., Van Morkhoven et al., 1986; Alegret et al., 2001, 2003). The bathymetric divisions defined in Van Morkhoven et al. (1986) have been followed: upper bathyal = 200–600 m, middle bathyal = 600–1000 m, lower bathyal = 1000–2000 m, and abyssal = >2000 m.

RESULTS

Paleobathymetry

The planktic-benthic foraminiferal ratio is very high (90%–95%) in most of the studied samples (except for those affected by dissolution in the lowermost Eocene), indicating open-ocean environments. Benthic forms can be used as accurate paleobathymetric markers because their distribution in the oceans is controlled by a series of depth-related parameters (e.g., Van Morkhoven et al., 1986; Kaminski and Gradstein, 2005). The mixed calcareous-agglutinated assemblages indicate deposition above the CCD for most of the studied section. Calcareous-cemented species (e.g., *Clavulinoides amorpha*, *C. globulifera*, *C. trilatera*, *Dorothia crassa*, *D. cylindracea*, *Gaudryina pyramidata*, *Marssonella floridana*, *Arenobulimina truncata*) and deep-water agglutinated foraminifera (DWAF) taxa (such as trochamminids, *Haplophragmoides*, *Karrerulina*, *Recurvoides*, and *Repmanina charoides*), are abundant in the studied samples. These assemblages are typical of the low to mid-latitude slope DWAF biofacies of Kuhnt et al. (1989). Among calcareous foraminifera, abundant representatives of the bathyal and abyssal Velasco-type fauna (Berggren and Aubert, 1975) include *Cibicidoides velascoensis*, *Gyroidinoides globosus*, *Nuttallides truempyi*, *Nuttallinella florealis*, *Osangularia velascoensis*, and others.

Assemblages are dominated by species that have an upper depth limit at the middle-upper bathyal boundary (500–700 m), such as *Bulimina trinitatensis*, *B. tuxpamensis*, *Buliminella grata*, *Nuttallides truempyi*, *Spiroplectammina spectabilis*, and *Stensioeina beccariiformis*. Other species, such as *Cibicidoides hyphalus*, *Gaudryina pyramidata*, *Gyroidinoides globosus*, and *Pullenia coryelli*, are most common at middle and lower bathyal depths (e.g.,

[1] www.paleo.ku.edu/palaios

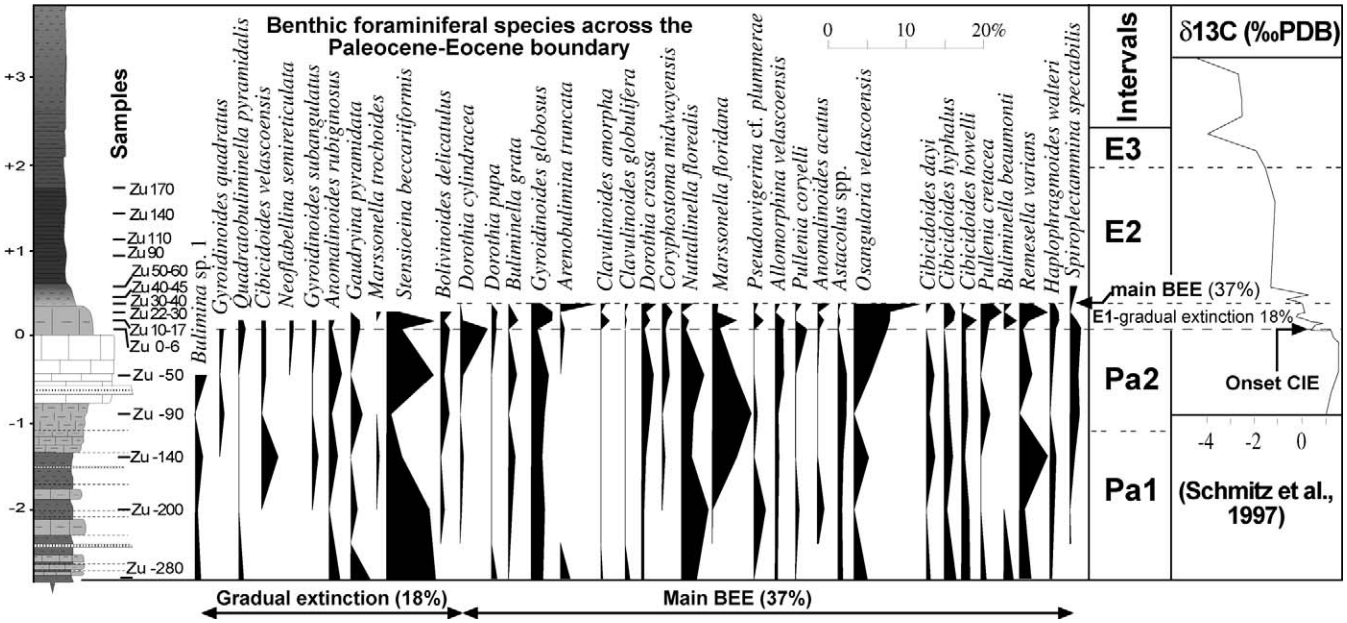

FIGURE 3—Stratigraphic distribution and relative abundance of benthic foraminiferal taxa that disappear in the lowermost Eocene in Zumaia and correlation to the $\delta^{13}C$ curve (in bulk sediment). BEE = benthic foraminiferal extinction event; CIE = carbon isotope excursion; PDB = Pee Dee Belemnite standard.

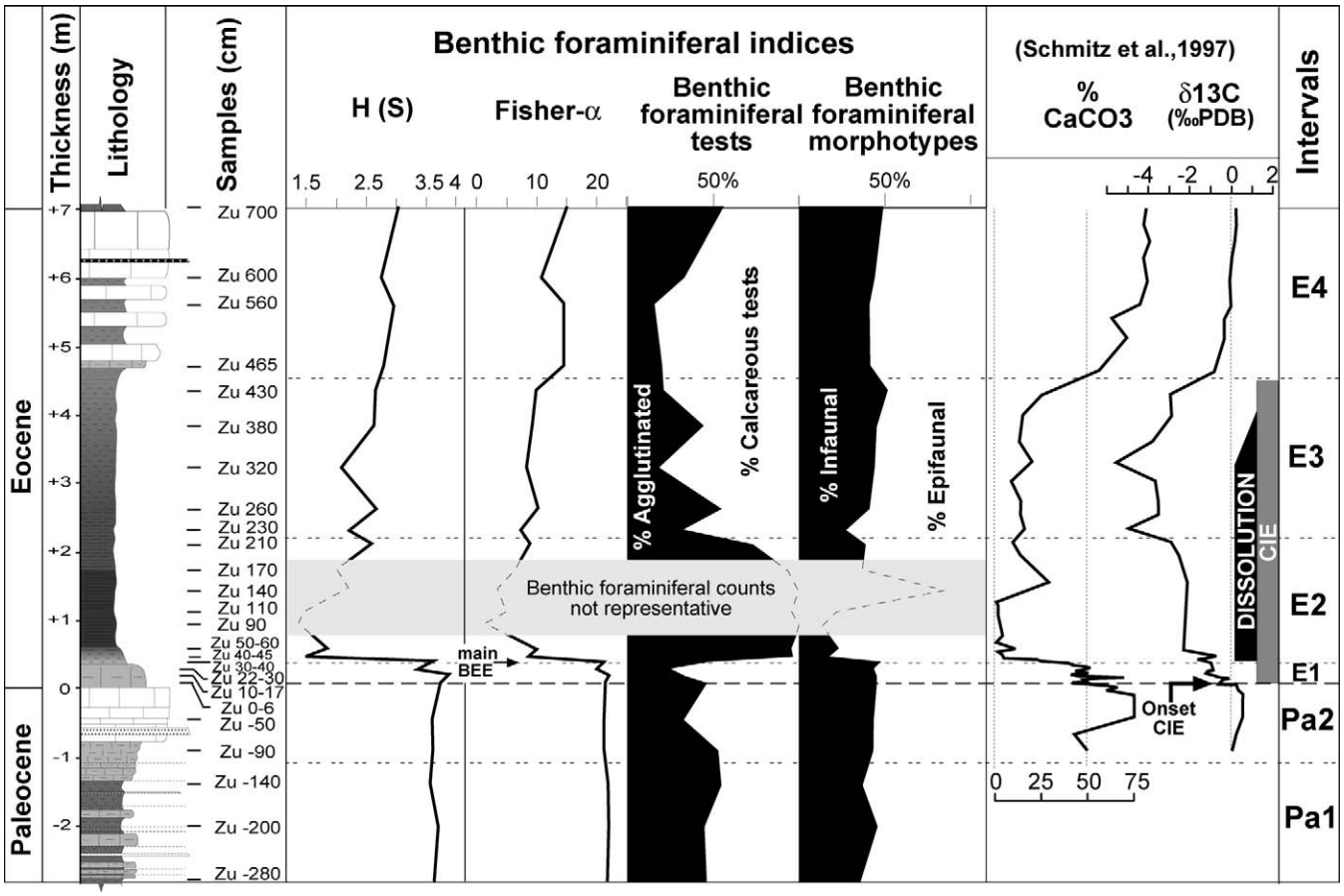

FIGURE 4—Benthic foraminiferal calcareous-agglutinated and infaunal-epifaunal ratios, heterogeneity and diversity indices, and $\delta^{13}C$ (in bulk sediment) and $\%CaCO_3$ values across the upper Paleocene and lower Eocene at Zumaia. H (S) = Shannon Weaver index of diversity; BEE = benthic foraminiferal extinction event; CIE = carbon isotope excursion; PDB = Pee Dee Belemnite standard.

Van Morkhoven et al., 1986; Alegret et al., 2003). These data, together with the occurrence of species that are common at upper and middle bathyal depths, such as *Angulogavelinella avnimelechi*, *Bolivinoides delicatulus*, or *Cibicidoides dayi*, suggest deposition close to the boundary between middle and lower bathyal environments (~1000 m depth).

These results agree with the wide depth range (600–1500 m) for deposition of these sediments given by Ortiz (1995) based on benthic foraminifera and with the paleobathymetry proposed by Pujalte et al. (1998), who used paleogeographical and sedimentary facies data to suggest that the uppermost Paleocene and lowermost Eocene sediments from Zumaia were deposited at ~1000 m depth. Our results also agree with depth estimates for the nearby Trabakua section (Orue-Etxebarria et al., 1996).

Microfossil Turnover

Previous study of marine microfossil assemblages of the Zumaia section, including benthic and planktic foraminifera and calcareous nannofossils, has evidenced the existence of significant biotic changes across the PETM. Considering these changes, we have divided the studied section into six distinctive intervals, Pa1–Pa2 and E1–E4 (Fig. 2), which are also characterized by changing values in both calcite concentration (%$CaCO_3$) and δC^{13}. Data on planktic foraminifera and calcareous nannofossils mainly come from previously published data sets (Orue-Etxebarria et al., 2004; Angori et al., 2007).

Interval Pa 1.—Benthic foraminiferal assemblages are very diverse (Fisher α = ~20), heterogeneous (H (S) = ~3.6), and consist of mixed infaunal (~37%–46% of the assemblages) and epifaunal (~54%–63%) morphogroups (Fig. 4). Infaunal morphogroups mainly consist of elongated-tapered (e.g., laevidentalinids, *Spiroplectammina navarroana*) and cylindrical-tapered (*Marssonella floridana*, *Remesella varians*) morphotypes. Epifaunal morphogroups are dominated by flattened trochospiral (trochamminids), biconvex trochospiral (*Anomalinoides ammonoides*, *Stensioeina beccariiformis*), and planoconvex trochospiral (*Nuttallides truempyi*, *Nuttallinella florealis*) morphotypes (Figs. 2, 3). Agglutinated foraminifera make up 44%–53% of the assemblages. Planktic foraminifera are very abundant within this interval, and their assemblages contain *Subbotina velascoensis*, *Morozovella occlusa*, *M. aequa*, *Acarinina soldadoensis*, *Globanomalina imitata*, and very rare *G. luxorensis* (<1% of the assemblages).

Calcareous nannofossil assemblages are characterized by abundant *Coccolithus pelagicus*, *Toweius pertusus*, and species of *Fasciculithus*, *Discoaster*, and *Sphenolithus*. Both abundance and species richness are high, with 40–50 species per sample and H (S) >2.1.

Interval Pa 2.—While no geochemical data are available from Pa1, relatively high %$CaCO_3$ and $\delta^{13}C$ values have been documented from the uppermost Paleocene sediments at Zumaia (Schmitz et al., 1997). This interval includes the uppermost 100 cm of the Paleocene comprising the green limestone interval.

Benthic foraminiferal assemblages are similar to those in Pa1, although the percentage of agglutinated taxa such as trochamminids slightly decreases, from 18%–26% in Pa1 to 11%–22% in Pa2. Epifaunal calcareous species such as *Anomalinoides ammonoides* or *Cibicidoides pseudoperlucidus* increase in relative abundance, especially toward the top of this interval. Planktic foraminiferal assemblages are also similar to those in Pa1, and the first occurrence of *Acarinina wilcoxensis*, *Globanomalina planoconica*, and *Planorotalites pseudoscitula* is recorded.

Changes in calcareous nannofossil assemblages have been used to distinguish Pa2 from Pa1. The boundary is marked by the beginning of a decreasing trend in the abundance and species richness of *Fasciculithus* and an increase in the abundance of *Zygrhablithus*. Although heterogeneity of the assemblages is still high (~2), fluctuations in the number of species per sample have been observed (36–51 species per sample).

A drop in %$CaCO_3$ values (from 75% to 50%) and a very minor decrease in $\delta^{13}C$ values are recorded in the uppermost ~20 cm of the Paleocene (Fig. 4), where the glauconite content is relatively high (Schmitz et al., 1997). No data on benthic and planktic foraminifera are available from this part of the section owing to its indurated nature, but nannofossil assemblages show a drop in the relative abundance and species richness of *Fasciculithus*, a slight decrease in abundance of *Discoaster* and *Sphenolithus*, and an increase in abundance of *Zygrhablithus* (Fig. 5).

Interval E1.—This marlstone interval marks the lowermost Eocene, and its base coincides with the onset of the carbon isotope excursion that marks the PE boundary, with a decrease in %$CaCO_3$ (~45% to ~25%). The diversity and heterogeneity of benthic foraminiferal assemblages decreases slightly compared to the Paleocene (Fig. 4), and the highest occurrence of 18% of the species, including *Stensioeina beccariiformis* at 22–30 cm above the boundary, is recorded within this interval. Calcareous benthic taxa, such as *Cibicidoides pseudoperlucidus*, *Lenticulina* spp., *Nuttallides truempyi*, *Osangularia velascoensis*, and *Pullenia jarvisi*, make up 52%–75% of the assemblages (Fig. 4). Their tests are well preserved, and there is no evidence of corrosion.

Among planktic foraminifera, Orue-Etxebarria et al. (2004) did not find any drastic changes in the assemblages or any extinctions. Among calcareous nannofossils, this interval is marked by an increase in the abundance of *Discoaster* (mainly *D. multiradiatus* and rare *D. nobilis*, *D. delicatus*, and *D. falcatus*) and *Fasciculithus* (mainly *F. tympaniformis* and rare *F.* cf. *hayii* and *F. thomasii*) and a sharp decrease in the abundance of *Zygrhablithus*.

Interval E2.—The highest occurrence of 37% of the benthic foraminiferal species (the main BEE) is placed at the boundary of E1 and E2 (sample Zu 30–40; see Fig. 3), which is at the base of the siliciclastic unit. Some of the species that have their highest occurrence at this level—such as *Arenobulimina truncata*, *Clavulinoides globulifera*, *Cribrostomoides trinitatensis*, *Dorothia pupa*, *Marssonella trochoides*, or *Remesella varians* among the agglutinated foraminifera and *Anomalinoides acutus*, *A. rubiginosus*, *Bolivinoides delicatulus*, *Buliminella grata*, *Cibicidoides dayi*, *C. hyphalus*, *C. velascoensis*, *Coryphostoma midwayensis*, *Gyroidinoides globosus*, *G. quadratus*, *G. subangulatus*, *Neoflabellina semireticulata*, *Nuttallinella florealis*, *Osangularia velascoensis*, or *Pullenia coryelli* among the calcareous ones—have been documented as becoming extinct globally (e.g., Tjalsma and Lohmann, 1983; Van Morkhoven et al., 1986; Thomas, 1990; Bolli et al., 1994; Kaminski and Gradstein, 2005). A single specimen of *R. varians* was found 20 cm above the BEE, but it is considered to be reworked. After the main BEE, diversity and heterogeneity of the assemblages reached the lowest values in the section (Fig. 4). Among calcareous nannofossils, the boundary between E1 and E2 is characterized by high percentages of *Discoaster* (mainly *D. multiradiatus*) and *Fasciculithus* (mainly *F. tympaniformis*) and very low percentages of *Zygrhablithus*.

A ~4-m-thick dissolution interval has been identified at Zumaia just above the BEE (Figs. 2, 4). Dissolution is more severe in the lower half of E2, where microfossil assemblages are dominated by agglutinated tests and very scarce, partially corroded calcareous foraminifera.

The main drop in %$CaCO_3$ is recorded at the base of interval E2, which is characterized by %$CaCO_3$ values of ~0%–10% in the lower 70 cm and ~20% toward the upper part (Fig. 4). Microfossil assemblages are strongly affected by dissolution, and calcareous benthic and planktic microfossils are very scarce or even absent. The only calcareous benthic specimens are scarce, thick-walled, dissolution-resistant forms such as buliminids and thick *Cibicidoides*.

Changes in total abundance of agglutinated benthic foraminifera are observed among the six samples studied from interval E2. Only the lowermost sample (Zu 50–60) contains sufficient specimens (>300) for quantitative analyses; 283 specimens were found in the uppermost sample (Zu 210; see Supplementary Data[1]). The benthic foraminiferal counts of the other samples are not reliable because they are not representative, although they can be studied qualitatively. The assemblages are strongly dominated by trochamminids (55%); *Recurvoides* (5%–16%), *Karrerulina*, *Haplophragmoides*, and *Repmanina charoides* are minor components (Fig. 2). Only one sample (Zu 140) is dominated by *Karrerulina* (*K. conversa* and *K. horrida*; 37% of the assemblages) instead of trochamminids.

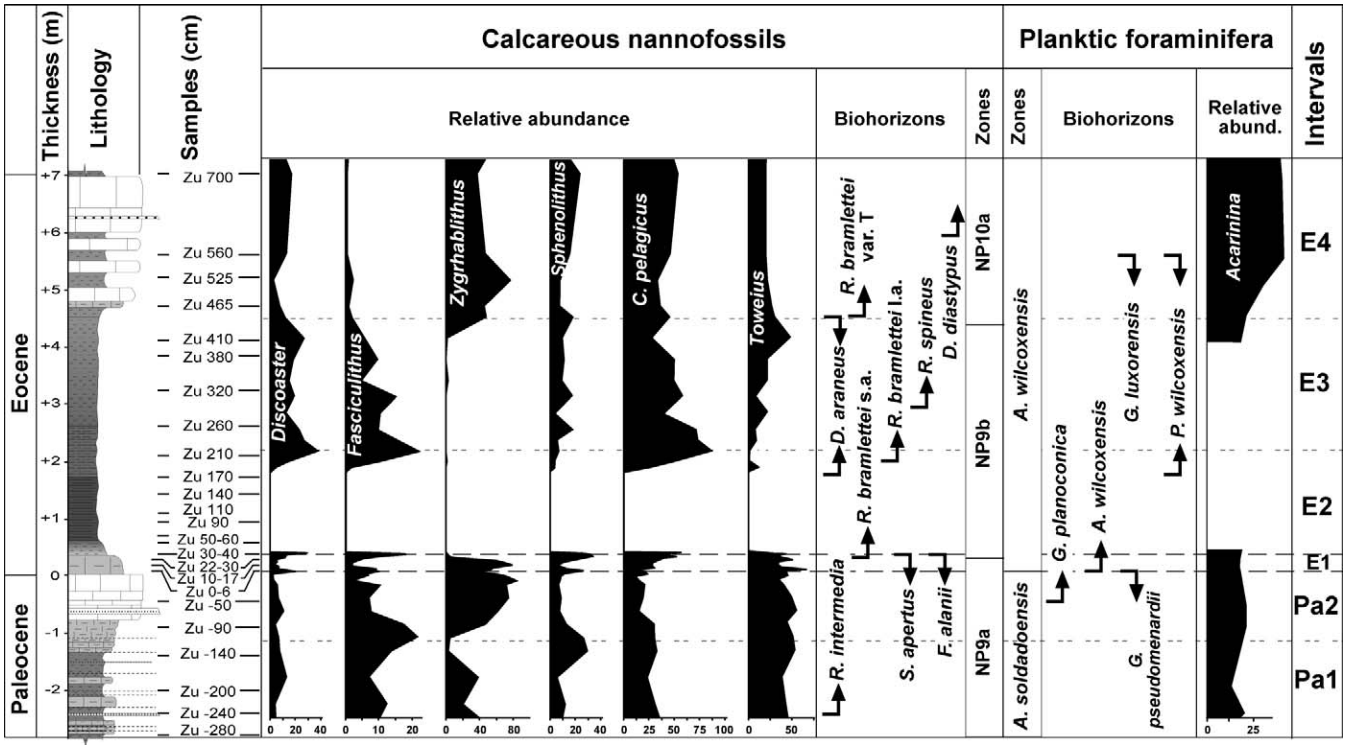

FIGURE 5—Calcareous nannofossil and planktic foraminifera main bioevents, biostratigraphic scheme, and relative abundance of selected taxa across the Paleocene–Eocene transition at the Zumaia section. Percentages of *Zygrhablithus*, *Fasciculithus*, and *Discoaster* are calculated from the non-*Toweius*+*Cocolithus pelagicus* fraction. Abbreviated genus names include: *C.* = *Coccolithus pelagicus*; *D.* = *Discoaster*; *R.* = *Rhomboaster*; *S.* = *Sphenolithus*; *F.* = *Fasciculithus*; *A.* = *Acarinina*; *G.* = *Globanomalina*; *P.* = *Planorotalites*. s.a. = short arms; l.a. = long arms; T = T-shape.

Whereas the lower 70 cm of interval E2 are almost devoid of calcareous microfossils, the upper part contains higher numbers of planktic (Canudo et al., 1995; Arenillas and Molina, 2000; Orue-Etxebarria et al., 2004) and calcareous benthic foraminiferal tests (e.g., *Bulimina tuxpamensis* and *Cibicidoides* in the >100 μm fraction and common *Tappanina selmensis* in the 63–100 μm fraction); these, however, are badly preserved and partially dissolved.

Interval E3.—This interval is characterized by $CaCO_3$ values of ~20% and minimum values of $\delta^{13}C$ (Fig. 4), although such negative values are possibly the result of diagenesis (Schmitz et al., 1997).

Interval E3 represents the upper half of the siliciclastic unit (Figs. 2, 4). Benthic foraminiferal assemblages are dominated by calcareous taxa with badly preserved, partially corroded tests. The effects of corrosion decrease toward the uppermost part of the interval. Assemblages are dominated by *Nuttallides truempyi*, *Globocassidulina subglobosa*, *Bulimina tuxpamensis*, *Cibicidoides pseudoperlucidus*, and *Oridorsalis umbonatus* among calcareous taxa and by trochamminids and *Repmanina charoides* (usually reported as *Glomospira*) among agglutinated taxa (Fig. 2). The species *Aragonia aragonensis* and *Abyssammina quadrata* reach their maximum relative abundance within this interval. Several calcareous, so-called Lazarus taxa that had temporarily disappeared at or just before the main BEE (e.g., *Abyssammina quadrata*, *Anomalinoides ammonoides*, *Cibicidoides ekblomi*, and *Lenticulina* spp.) reappear within this interval, and *Nonion havanense* first occurs. The diversity and heterogeneity of the assemblages slightly increase across interval E3, although these values are still low (Fig. 4).

The abundance of planktic foraminiferal tests increases in this interval, and the last occurrence of *G. chapmani* is recorded (Orue-Etxebarria et al., 2004). Calcareous nannofossils are characterized by the presence of the *Rhomboaster-Discoaster araneus* assemblage, and the highest percentages of *Coccolithus pelagicus*, *Fasciculithus*, and *Discoaster* spp. occur in this interval (Fig. 5).

Interval E4.—The recovery of $\%CaCO_3$ and $\delta^{13}C$ levels to preexcursion values occurred within this interval, which includes a succession of well-defined, limestone-marl couplets (Fig. 4). Benthic foraminiferal assemblages are dominated by calcareous taxa (80%), mainly by *Nuttallides truempyi*, though *Bulimina tuxpamensis*, *Cibicidoides pseudoperlucidus*, *C. ekblomi*, and *Oridorsalis umbonatus* are also abundant (Fig. 2). Except for *O. umbonatus*, the percentages of the other species above, and of calcareous taxa, decrease in the uppermost sample (Zu 700), where assemblages contain 56% of agglutinated taxa, the same as in the upper Paleocene. Among agglutinated foraminifera, trochamminids, *Repmanina charoides*, and *Karrerulina* are the most abundant taxa; *Recurvoides* is also common in this interval, and several Lazarus taxa, such as *Hyperammina dilatata* and *Pullenia jarvisi*, reappear. Benthic foraminiferal assemblages gradually recover across this interval, as inferred from their increased heterogeneity and diversity, although these values are lower than preextinction values (Fig. 4).

Among planktic foraminifera, the genus *Acarinina* strongly dominates the assemblages within this interval (Orue-Etxebarria et al., 2004). In calcareous nannofossil assemblages (Fig. 5), abundance and species richness increases. The percentage of *Zygrhablithus* increases considerably, becoming one of the most abundant taxa together with *C. pelagicus* and *Toweius*, whereas *Discoaster* and *Fasciculithus* decrease in relative abundance, and the *Rhomboaster-Discoaster araneus* assemblage is no longer present (Bernaola et al., 2006).

DISCUSSION

Paleoenvironmental Reconstruction at Zumaia

Upper Paleocene (Pa1) benthic foraminiferal assemblages indicate mesotrophic conditions at the seafloor, with enough nutrient flux to the seafloor to sustain both infaunal and epifaunal species (Jorissen et al., 1995). The high percentage of agglutinated foraminifera indicates a considerable

input of fine-grained clastic material. A high detrital flux has been documented for the upper Paleocene in Zumaia and in nearby sections of the western Pyrenees (Orue-Etxebarria et al., 1996; Kuhnt and Kaminski, 1997; Pujalte et al., 1998; Baceta et al., 2000; Schmitz et al., 2000; Bernaola et al., 2006). Calcareous nannofossil assemblages indicate stable oceanic conditions, with a stratified water column and a low-nutrient content (Bernaola et al., 2006).

This period of stable conditions was followed by an initial perturbation phase in surface waters (interval Pa2), which preceded the CIE and the main warming event of the PETM. Fluctuations in the species richness and in the percentage of calcareous nannofossil taxa in interval Pa2 indicate the onset of the environmental perturbation, with an expansion of low-latitude, warm-water assemblages to high latitudes, probably caused by an abrupt increase in surface water temperatures (Bernaola et al., 2006), and an elevated nutrient supply in surface waters, possibly caused by increased upwelling or nutrient runoff. This initial perturbation phase is considered to have started about 46 kyr before the onset of the CIE, based on the fact that interval Pa2 is ~115 cm thick and assuming an average sedimentation rate for the uppermost Paleocene of ~2.5 $cm \cdot kyr^{-1}$ (Dinarès-Turell et al., 2007).

The benthic foraminiferal changes, and the gradual but rapid extinction of 18% of the species (minimizing the Signor-Lipps effect), point to an early perturbation of the seafloor between the onset of the CIE and the main BEE (interval E1; see Fig. 3). Although the extinction of *S. beccariiformis* has been related to the BEE (Thomas, 1998), this species may have become extinct earlier, at least locally, at other locations such as the Basque-Cantabrian Basin (e.g., Schmitz et al., 1997).

The main BEE, which includes the disappearance of 37% of the species at Zumaia, coincided with a rapid increase in relative abundance of agglutinated foraminifera. One might assume that dissolution was the only cause of the BEE and the dominance of agglutinated taxa; however, 18% of the benthic foraminiferal species, following a gradual pattern, disappeared below the main BEE and the dissolution interval (Fig. 2), suggesting that dissolution was not the only cause of the extinctions. Because 18% of the benthic species became extinct within interval E1, and the main BEE (37%) occurred at its top, we conclude that the benthic foraminiferal extinction event was gradual but rapid, affecting 55% of the species in total, which is in line with deep-sea records of the BEE (30%–50%; e.g., Tjalsma and Lohmann, 1983; Kaiho, 1994; Thomas, 1998, 2007). Its duration corresponds to interval E1. Assuming a duration of ~105 kyr (Giusberti et al., 2007; Röhl et al., 2007) for the core of CIE, which at Zumaia is represented by the siliciclastic unit, an average sedimentation rate of 3.8 $cm \cdot kyr^{-1}$ can be inferred for the CIE interval at this section. As interval E1 is 40 cm thick, it may represent ~10.5 kyr. Therefore, it may be concluded that the gradual extinction event recorded within interval E1 was geologically very rapid, lasting for ~10.5 kyr.

The common occurrence of *C. pseudoperlucidus* (Fig. 2) in interval E1 suggests oxic conditions at the seafloor. This species is large, thick-walled, and multichambered, in contrast to the typical low-oxygen, r-selected morphotypes, which generally have few chambers, small tests, and thin walls (Bernhard, 1986).

A ~4-m-thick interval characterized by enhanced dissolution has been identified at Zumaia just above the BEE (intervals E2 and E3; see Figs. 2, 4). Dissolution was more severe in E2, where microfossil assemblages are dominated by DWAF taxa that are very common in sediments deposited beneath the lysocline (Kaminski and Gradstein, 2005), supporting a sudden rise in the CCD, and very scarce, partially corroded calcareous foraminifera. Benthic foraminiferal assemblages from the upper half of the dissolution interval are mainly dominated by calcareous taxa (especially *N. truempyi*; see Figs. 2, 4), although their tests are strongly corroded. The effects of corrosion decrease toward the uppermost part of interval E3. According to Schmitz et al. (2000), sedimentation rates for siliciclastic material increased during deposition of the siliciclastic unit, reflecting a significant change in climate and hydrological regime toward a warmer (in agreement with the calcareous nannofossil record) and seasonally drier climate. We therefore suggest that low $\%CaCO_3$ at Zumaia resulted not only from dissolution, which strongly affected calcareous foraminiferal tests within the SU, but also from dilution of carbonate-rich material by terrigenous matter—as indicated by a significant increase in the estimated sedimentation rates from interval Pa2 to the siliciclastic unit (from 2.5 to 3.8 $cm \cdot kyr^{-1}$)—and possibly a large influx of refractory organic matter from land (Schmitz and Pujalte, 2007).

The abundance of several species of *Ammodiscus*, *Glomospira*, and *Glomospirella* in interval E3 may correspond to the event commonly called the *Glomospira* acme, which has been recognized in the lowermost Eocene at various locations (see references in Kaminski and Gradstein, 2005). Recent species of *Ammodiscus*, *Glomospira*, *Glomospirella*, and *Repmanina* are mobile epifaunal forms that feed on organic detritus (e.g., Ly and Kuhnt, 1994) and tolerate large environmental fluctuations, including variations in salinity and oxygenation (e.g., Kaminski et al., 1996). Among calcareous nannofossils, maximum values in the percentages of *Coccolithus pelagicus*, *Fasciculithus*, and *Discoaster* spp. within interval E3 (Fig. 5) are likely controlled by water temperature (Orue-Etxebarria et al., 2004). According to these authors, the disappearance of *Zygrhablithus bijugatus*, a species thought to indicate oligotrophic conditions, may result from increased productivity in the water column due to a higher nutrient supply, a situation that agrees with increased continental erosion in the Basque basin as suggested by Schmitz et al. (2000). Such increased erosion might account for the common occurrence of opportunistic benthic foraminiferal species, such as the *Glomospira* acme and abundant trochamminids, as well as *Karrerulina*, *Recurvoides*, and *Haplophragmoides* in intervals E2 and E3. These taxa may have taken advantage of a high-stress, probably strongly fluctuating environment, with rapidly changing seafloor conditions (Sliter, 1975; Koutsoukos et al., 1991; Ly and Kuhnt, 1994; Kaminski et al., 1996; Kuhnt et al., 1996; Gooday, 2003).

According to Ortiz (1995), the dominance of finely agglutinated (*Haplophragmoides*, *Glomospira*) and calcareous epifaunal taxa (*N. truempyi*) after the extinction event points to low-oxygen conditions for the lowermost 22 m of the Eocene at Zumaia. Many agglutinated and calcareous taxa that are abundant in the lower Eocene at Zumaia, however, tolerate large environmental fluctuations, and there is no clear independent evidence for dysoxia. The occurrence of very abundant and partially corroded tests of *N. truempyi* in the lower half of interval E3 may indicate corrosive bottom waters, as does its homeomorph descendant, *N. umbonifera* (Jorissen et al., 2007). The maximum abundances of *Bulimina tuxpamensis* and *T. selmensis* in intervals E2 and E3 may be related to both low-oxygen and high-nutrient conditions (Olsson and Wise, 1987; Thomas, 1990; Gibson et al., 1993; Sen Gupta and Machain-Castillo, 1993; Steineck and Thomas, 1996; Bernhard et al., 1997). *Tappanina selmensis* may also indicate stressed seafloor conditions with undersaturated bottom waters (Boltovskoy et al., 1991; Takeda and Kaiho, 2007), whereas *R. charoides* appears to be opportunistic and independent of oxygen levels (Kaminski et al., 1996; Kaminski and Gradstein, 2005). The high percentages of *Globocassidulina subglobosa* ($\leq$17.6% of the assemblages), an oxic indicator (Schönfeld, 2001; Martins et al., 2007), and the common occurrence of *C. pseudoperlucidus*, a typical oxic species with a thick-walled test and large pores, however, point to oxic conditions at the seafloor during interval E3. In addition, the reddish color of the SU suggests well-oxygenated bottom waters that were able to oxidize minerals from the SU. A peak in the percentage of *Aragonia aragonensis* is also recorded within interval E3; this species is common in postextinction intervals at several ODP Sites (e.g., Thomas, 1998, 2003) and has been suggested as an opportunistic species (Steineck and Thomas, 1996).

The paleoecological affinities of the calcareous nannofossil *Rhomboaster-Discoaster araneus* assemblage, which dominates within interval E3, are unknown (e.g., Bralower, 2002; Agnini et al., 2006; Bernaola et al., 2006). According to Egger et al. (2005), this assemblage indicates ecological perturbations in oceanic surface waters developed during the CIE

interval. The co-occurrence of this short-lived association with *Thoracosphaera* suggests that stressed surface-water conditions (Gibbs et al., 2006; Agnini et al., 2007) prevailed during interval E3, whereas benthic foraminifera indicate oxic and rapidly changing seafloor conditions, possibly related to increased continental erosion and a large flux of organic matter from land (Schmitz and Pujalte, 2007). Alternatively, the appearance of asymmetrical *Discoaster* and *Rhomboaster* species might indicate the development and availability of new ecological niches, resulting from major paleoceanographic changes during the PETM (Bralower, 2002).

We suggest that the sharp transition in lithology from the siliciclastic unit to the overlying limestone-marl couplets, coincident with a shift toward heavier $\delta^{13}C$ values, indicates a sudden stop in the weathering of continental silicates at the top of the SU. The calcareous nannofossil turnover and the increase in the percentage of acarininids (Orue-Etxebarria et al., 2004) in interval E4 at Zumaia have been related to a sea-level rise that displaced the shoreline >10 km landward, flooding vast continental areas in the Basque Basin (Baceta, 1996). This sea-level rise led to the sequestration of nutrients in shelf environments; the consecutive relative starvation of surface waters in the open ocean might have triggered nannofossil turnover owing to a shift to more oligotrophic conditions (Orue-Etxebarria et al., 2004). The recovery of $\%CaCO_3$ and $\delta^{13}C$ to preexcursion values is recorded within interval E4. A typical postextinction, benthic foraminiferal fauna with *N. truempyi* and *O. umbonatus* occurs in this interval, as it does in ODP sites (e.g., Thomas and Shackleton, 1996). The low diversity and heterogeneity of the assemblages indicate that environmental conditions, including the flux of organic carbon, had not completely recovered at the top of the studied section.

Turnover and Timing

The rapid injection of ^{13}C-depleted carbon at the PE boundary was preceded by environmental perturbation in surface waters at Zumaia. Calcareous nannofossils indicate a period (interval Pa2) of gradual surface-water warming previous to the onset of the CIE; assuming an average sedimentation rate of 2.5 $cm \cdot kyr^{-1}$ for the uppermost Paleocene at Zumaia (Dinarès-Turell et al., 2007), environmental changes in surface waters started ~46 kyr before the onset of the CIE at Zumaia. A similar faunal turnover has been observed in other Tethyan sections as well as at high latitudes (Angori et al., 2007) and indicates a shift from cold-water to warm-water taxa caused by a sudden expansion of low-latitude, warm-water assemblages to high latitudes, as a result of an abrupt increase in surface-water temperatures. A ~2° C warming of surface waters has been observed <10 kyr before the onset of the CIE at different paleogeographical locations (Thomas et al., 2002; Sluijs et al., 2007b) and is consistent with the hypothesis that methane hydrate dissociation was triggered by bottom-water warming during the latest Paleocene. This warming, however, does not rule out other models for methane release (i.e., thermogenic) or biomass burning (e.g., Moore and Kurtz, 2008). The difference in timing (46 kyr at Zumaia vs. <10 kyr at some other sites) remains to be explained, although changing seafloor conditions have been recently observed during the last 45 kyr of the Paleocene in the Italian Contessa Road section (Giusberti et al., 2009).

The release of methane and the increase in concentration of its oxidation product CO_2 (and its dissolution in sea water) during the early stage of warming could have accounted for the intense dissolution in the deep sea, although the occurrence of severe dissolution at shallow settings, however, is not expected by carbon-cycle modeling (e.g., Dickens et al., 1997; Thomas, 2007). In deep-water settings such as Zumaia and the Italian Forada section (Giusberti et al., 2007), preservation of carbonate improves gradually up section in the siliciclastic unit, which is consistent with an abrupt and rapid acidification of the oceans followed by a slower deepening of the CCD.

Just above the onset of the CIE, microfossil data from Zumaia support a gradual but rapid onset of the PETM, followed by long-term effects on calcareous nannoplankton as well as on benthic foraminiferal assemblages. Changes in calcareous nannofossil assemblages and the disappearance of 18% of the benthic foraminiferal species between the onset of the CIE and the main BEE indicate perturbation at the seafloor and in surface waters, as documented from other Tethyan localities (e.g., Pardo et al., 1999; Galeotti et al., 2005; Angori et al., 2007). This gradual but rapid initiation of the paleoecological and paleoceanographic turnover eventually led to the main BEE, about 10.5 kyr after the onset of the CIE.

Causes of the Benthic Foraminiferal Extinctions

Benthic foraminiferal turnover and extinctions occur globally across the PETM, and therefore they must have a global cause. Dissolution may have caused some extinctions locally, but it was not global (e.g., Thomas et al., 1999; Gibbs et al., 2006; John et al., 2008). At Zumaia, a gradual extinction of 18% of the species is recorded below the dissolution interval, suggesting that dissolution was not the (only) cause of the BEE and the benthic foraminiferal turnover. Moreover, refugia should have existed for carbonate corrosivity, since the dramatic decrease in carbonate percentage is not recorded globally (Takeda and Kaiho, 2007; Thomas, 2007). Decreased oxygenation of bottom waters might have been another cause that triggered the BEE, although the gradual extinction of benthic foraminifera has been recorded at Zumaia across an interval with inferred oxic conditions. Low-oxygen conditions have been well documented in marginal ocean basins such as the Tethys (e.g., Speijer and Wagner, 2002; Alegret et al., 2005; Alegret and Ortiz, 2006) and northeastern peri-Tethys (e.g., Gavrilov et al., 2003), but the record for open-ocean settings is not so clear; even if locally the oceans were hypoxic or anoxic, some regions should have remained suitable for benthic foraminifera, which have considerable tolerance for low-oxygen levels. It seems unlikely that productivity changes in surface waters could have caused a major benthic extinction because deep-sea benthic foraminifera survived global environmental crises such as the asteroid impact at the end of the Cretaceous without significant extinction (e.g., Alegret and Thomas, 2005; Alegret, 2007). The primary producer community was unstable during the PETM (e.g., Bralower, 2002; Bernaola et al., 2006), however, and probably involved changes in the food flux (type, quantity) to the seafloor, thus triggering changes in the benthic communities and blooms of opportunistic benthic foraminifera, which may have taken advantage of a high-stress, probably strongly fluctuating environment (e.g., Katz et al., 1999). Locally, nutrient flux to the seafloor may have fluctuated at Zumaia owing to increased influx of refractory organic matter from land (which might not be easily used by many benthic foraminiferal species) and high seasonal precipitation (Schmitz and Pujalte, 2007).

According to Thomas (2007), warming may have been the global feature of the PETM that triggered the global extinction of benthic foraminifera, since it has been recorded at all investigated latitudes and oceans. This author hypothesized the possible effects of global warming on oceanic ecosystems, which would include changes in energy cycling within ecosystems, possibly affecting productivity by calcareous nannoplankton, changes in the rate of evolutionary processes, and even fluctuations in the compounds and amount of labile organic matter available for foraminiferal feeding. These changes in oceanic ecosystems may have started at Zumaia after the initial warming phase of the surface waters inferred for the last 46 kyr of the Paleocene (as compared to the last ~3–5 kyr of the Paleocene at some other locations; see Sluijs et al., 2007b), thus triggering the benthic foraminiferal turnover and extinctions that occurred over a geologically rapid (~10.5 kyr) period of time.

CONCLUSIONS

The effects of the PETM have been analyzed in the Zumaia section based on the study of benthic and planktic foraminifera and calcareous nannofossils. Microfossil data from Zumaia support a rapid onset of the PETM, followed by long-term effects on calcareous nannoplankton as well as in benthic foraminiferal assemblages.

Calcareous nannofossils indicate initial warming of surface waters during the latest Paleocene, ~46 kyr before the onset of the CIE. Initial warming may have increased the hydrological cycle, leading to increased flux of terrestrial matter from land. The BEE was gradual but rapid, with a duration of ~10,5 kyr, and affected 55% of the species at Zumaia. The gradual disappearance of 18% of the benthic foraminiferal species previous to the main BEE suggests that environmental conditions at the seafloor were significantly disturbed at the beginning of the Eocene. The gradual extinction of 18% of the species occurred under inferred oxic conditions without evidence for calcareous dissolution, indicating that carbonate corrosivity and oxygenation of the bottom waters were not the main cause. Warming may have been the only global feature of the PETM for which there were no refugia, and the initial warming phase recorded during the latest Paleocene must have triggered paleoecological and paleoenvironmental instability, leading to the gradual but rapid BEE.

A dissolution interval occurs above the main BEE, indicating that bottom waters became corrosive after the main extinction. Low $\%CaCO_3$ at Zumaia, however, resulted not only from dissolution but also from dilution of carbonate-rich material by terrigenous matter and possibly a large influx of refractory organic matter from land. The gradual recovery of isotopic levels and the improved preservation of carbonate toward the top of the siliciclastic unit at Zumaia are consistent with a slow deepening of the CCD after the initial, abrupt acidification of the oceans. The sharp transition in lithology from the SU to the overlying limestone-marl couplets points to a sudden stop in the weathering of continental silicates. The recovery of $\%CaCO_3$ and $\delta^{13}C$ to preexcursion values is recorded above the SU, where the calcareous plankton point to sea-level rise and oligotrophic conditions in surface waters, whereas benthic foraminifera indicate that environmental conditions (flux of organic carbon, or possibly the type of organic matter) had not completely recovered at the top of the studied section.

ACKNOWLEDGMENTS

We are grateful to Mimi Katz, Ellen Thomas, and the Editor and Associate Editor of PALAIOS for their helpful reviews, which significantly improved this manuscript. We acknowledge the Spanish Ministry of Science and Technology for two Ramón y Cajal research contracts to L. Alegret and J.I. Baceta and a postdoctoral grant EX2007-1094 to S. Ortiz. This research is a contribution to Projects CGL2005-01721BTE and CGL2007-63724 (Ministry of Science and Technology, Spanish Government).

REFERENCES

Agnini, C., Fornaciari, E., Rio, D., Tateo, F., Backman, J., and Giusberti, L., 2007, Responses of calcareous nannofossil assemblages, mineralogy and geochemistry to the environmental perturbations across the Paleocene/Eocene boundary in the Venetian Pre-Alps: Marine Micropaleontology, v. 63, p. 19–38.

Agnini, C., Muttoni, G., Kent, D.V., and Rio, D., 2006, Eocene biostratigraphy and magnetic stratigraphy from Possagno, Italy: The calcareous nannofossil response to climate variability: Earth and Planetary Science Letters, v. 241, p. 815–830.

Alegret, L., 2007, Recovery of the deep-sea floor after the Cretaceous-Paleogene boundary event: The benthic foraminiferal record in the Basque–Cantabrian basin and in South-eastern Spain: Palaeogeography, Palaeoclimatology, Palaeoecology, v. 255, p. 181–194.

Alegret, L., Molina, E., and Thomas, E., 2001, Benthic foraminifera at the Cretaceous/Tertiary boundary around the Gulf of Mexico: Geology, v. 29, p. 891–894.

Alegret, L., Molina, E., and Thomas, E., 2003, Benthic foraminiferal turnover across the Cretaceous/Paleogene boundary at Agost (southeastern Spain): Paleoenvironmental inferences: Marine Micropaleontology, v. 48, p. 251–279.

Alegret, L., and Ortiz, S., 2006, Global extinction event in benthic foraminifera across the Paleocene/Eocene boundary at the Dababiya Stratotype section: Micropaleontology, v. 52, p. 433–447.

Alegret, L., Ortiz, S., Arenillas, I., and Molina, E., 2005, Paleoenvironmental turnover across the Palaeocene/Eocene boundary at the Stratotype section in Dababiya (Egypt) based on benthic foraminifera: Terra Nova, v. 17, p. 526–536.

Alegret, L., and Thomas, E., 2005, Cretaceous/Paleogene boundary bathyal paleoenvironments in the central North Pacific (DSDP [Deep Sea Drilling Project] Site 465), the Northwestern Atlantic (ODP [Ocean Drilling Program] Site 1049), the Gulf of Mexico and the Tethys: The benthic foraminiferal record: Palaeogeography, Palaeoclimatology, Palaeoecology, v. 224, p. 53–82.

Angori, E., Bernaola, G., and Monechi, S., 2007, Calcareous nannofossil assemblages and their response to the Paleocene–Eocene Thermal Maximum event at different latitudes: ODP [Ocean Drilling Program] Site 690 and Tethyan sections, *in* Monechi, S., Coccioni, R., and Rampino, M., eds., Large Ecosystem Perturbations: Causes and Consequences: Geological Society of America Special Paper no. 424, p. 69–85.

Arenillas, I., and Molina, E., 1996, Bioestratigrafía y evolución de las asociaciones de foraminíferos planctónicos del Tránsito Paleoceno–Eoceno en Alamedilla (Cordilleras Béticas): Revista Española de Micropaleontología, v. 28, p. 75–96.

Arenillas, I., and Molina, E., 2000, Reconstrucción paleoambiental con foraminíferos planctónicos y cronoestratigrafía del tránsito Paleoceno–Eoceno de Zumaya (Guipúzcoa): Revista Española de Micropaleontología, v. 32, p. 283–300.

Aubry, M.P., 1995, From Chronology to Stratigraphy: Interpreting the Lower and Middle Eocene Stratigraphic Record in the Atlantic Ocean: SEPM (Society for Sedimentary Geology) Special Publication, Tulsa, Oklahoma, v. 54, p. 213–274.

Aubry, M.P., Ouda, K., Dupuis, Ch., Berggren, W.A., Van Couvering, J.A., and the Members of the Working Group on the Paleocene/Eocene Boundary, 2007, The Global Standard Stratotype-Section and Point (GSSP) for the base of the Eocene Series in the Dababiya section (Egypt): Episodes, v. 30, p. 271–286.

Baceta, J.I., 1996, El Maastrichtiense superior, Paleoceno e Ilerdiense inferior de la región Vasco-Cantábrica: Secuencias deposicionales, facies y evolución paleogeográfica: Unpublished Ph.D. disserataion, University of the Basque Country, Bilbao, Spain, p. 1–372.

Baceta, J.I., Pujalte, V., Dinarès-Turell, J., Payros, A., Orue-Etxebarria, X., and Bernaola, G., 2000, The Paleocene/Eocene boundary interval in the Zumaia Section (Gipuzkoa, Basque Basin): Magnetostratigraphy, and high-resolution lithostratigraphy: Revista de la Sociedad Geológica de España, v. 13, p. 375–391.

Baceta, J.I., Pujalte, V., Serra-Kiel, J., Robador, A., and Orue-Etxebarria, X., 2004, El Maastrichtiense final, Paleoceno e Ilerdiense inferior de la Cordillera Pirenaica, *in* Vera, J.A., ed., Geología de España: Sociedad Geológica de España, Instituto Geológico y Minero de España, Madrid, p. 308–313.

Balsam, W.L., and Beeson, J.P., 2003, Sea-floor sediment distribution in the Gulf of Mexico: Deep Sea Research Part I: Oceanographic Research Papers, v. 50, p. 1421–1444.

Berggren, W.A., and Aubert, J., 1975, Paleocene benthonic foraminiferal biostratigraphy, paleobiogeography and paleoecology of Atlantic-Tethyan regions: Midway-type fauna: Palaeogeography, Palaeoclimatology, Palaeoecology, v. 18, p. 73–192.

Bernaola, G., Angori, E., and Monechi, S., 2006, Calcareous nannofossil turnover across the P/E boundary interval, *in* Bernaola, G., Baceta, J.I., Payros, A., Orue-Etxebarria, X., and Apellaniz, E., eds., The Paleocene and Lower Eocene of the Zumaia Section (Basque Basin): Post-Conference Field Trip Guidebook, Conference on Climate and Biota of the Early Paleogene, 2006, Bilbao, Spain, p. 63–67, http://www.earth-prints.org/bitstream/2122/2299/1/993.pdf. Checked 21 January 2009.

Bernaola, G., Baceta, J.I., Orue-Etxebarria, X., Alegret, L., Martin, M., Arostegui, J., and Dinarès, J., 2007, Evidences of an abrupt environmental disruption during the mid-Paleocene biotic event (Zumaia section, W. Pyrenees): Geological Society of America Bulletin, v. 119, p. 785–795.

Bernhard, J.M., 1986, Characteristic assemblages and morphologies of benthic foraminifera from anoxic, organic-rich deposits: Jurassic through Holocene: Journal of Foraminiferal Research, v. 16, p. 207–215.

Bernhard, J.M., Sen Gupta, B.K., and Borne, P.F., 1997, Benthic foraminiferal proxy to estimate dysoxic bottom water oxygen concentrations, Santa Barbara Basin, US Pacific continental margin: Journal of Foraminiferal Research, v. 27, p. 301–310.

Bolli, H.M., Beckmann, J.P., and Saunders, J.B., 1994, Benthic Foraminiferal Biostratigraphy of the South Caribbean Region: Cambridge University Press, Cambridge, UK, 408 p.

Boltovskoy, E., Scott, D.B., and Medioli, F.S., 1991, Morphological variations of benthic foraminiferal tests in response to changes in ecological parameters, a review: Journal of Paleontology, v. 65, p. 175–185.

Bowen, G.J., Bralower, T.J., Delaney, M.L., Dickens, G.R., Kelly, D.C., Koch, P.L., Kump, L.R., Meng, J., Sloan, L.C., Thomas, E., Wing, S.L., and Zachos, J.C., 2006, The Paleocene–Eocene thermal maximum gives insight into greenhouse gas-induced environmental and biotic change, Eos, v. 87, p. 165–169.

Bralower, T.J., 2002, Evidence of surface water oligotrophy during the Paleocene–Eocene thermal maximum: Nannofossil assemblage data from Ocean Drilling Program Site 690, Maud Rise, Weddell Sea: Paleoceanography, v. 17, no. 2, p. 1023, doi: 10.1029/2001PA000662.

Canudo, J.I., Keller, G., Molina, E., and Ortiz, N., 1995, Planktic foraminiferal turnover and $\delta^{13}C$ isotopes across the Paleocene–Eocene transition at Caravaca and Zumaya, Spain: Palaeogeography, Palaeoclimatology, Palaeoecology, v. 114, p. 75–100.

Crouch, E.M., Heilmann-Clausen, H., Brinkhuis, H.E.G., Morgans, K.M., Rogers, H., Egger, B., and Schmitz, B., 2001, Global dinoflagellate event associated with the Paleocene thermal maximum: Geology, v. 29, p. 315–318.

Dickens, G.R., Castillo, M.M., and Walker, J.G.C., 1997, A blast of gas in the latest Paleocene: Simulating first-order effects of massive dissociation of oceanic methane hydrate: Geology, v. 25, p. 259–262.

Dickens, G.R., O'Neil, J.R., Rea, D.K., and Owen, R.M., 1995, Dissociation of oceanic methane hydrate as a cause of the carbon isotope excursion at the end of the Paleocene: Paleoceanography, v. 10, p. 965–971.

Dinarès-Turell, J., Baceta, J.I., Bernaola, G., Pujalte, V., and Orue-Etxebarria, X., 2007, Closing the mid-Palaeocene gap: Toward a complete astronomically tuned Palaeocene Epoch and Selandian and Thanetian GSSPs at Zumaia (Basque Basin, W Pyrenees): Earth and Planetary Science Letters, v. 262, p. 450–467.

Dinarès-Turell, J., Baceta, J.I., Pujalte, V., Orue-Etxebarria, X., and Bernaola, G., 2002, Magnetostratigraphic and cyclostratigraphic calibration of a prospective Paleocene/Eocene stratotype at Zumaia (Basque Basin, northern Spain): Terra Nova, v. 14, p. 371–378.

Egger, H., Homayoun, M., Huber, H., Rögl, F., and Schmitz, B., 2005, Early Eocene climatic, volcanic, and biotic events in the northwestern Tethyan Untersberg section, Austria: Palaeogeography, Palaeoclimatology, Palaeoecology, v. 217, p. 243–264.

Galeotti, S., Kaminski, M.A., Coccioni, R., and Speijer, R., 2005, High resolution deep water agglutinated foraminiferal record across the Paleocene/Eocene transition in the Contessa Road Section (Italy), *in* Bubik, M., and Kaminski, M.A., eds., Proceedings, Sixth International Workshop on Agglutinated Foraminifera: Grzybowski Foundation Special Publication no. 8, p. 83–103.

Gavrilov, Y.O., Shcherbinina, E.A., and Oberhänsli, H., 2003, Paleocene-Eocene boundary events in the northeastern Peri-Tethys: Geological Society of America Special Paper no. v. 369, p. 147–168.

Gawenda, P., Winkler, W., Schmitz, B., and Adatte, T., 1999. Climate and bioproductivity control on carbonate turbidite sedimentation (Paleocene to earliest Eocene, Gulf of Biscay, Zumaia, Spain): Journal of Sedimentary Research, v. 69, p. 1253–1261.

Gibbs, S.J., Bralower, T.J., Bown, P.R., Zachos, J.C., and Bybell, L.M., 2006, Shelf and open-ocean calcareous phytoplankton assemblages across the Paleocene–Eocene thermal maximum: Implications for global productivity gradients: Geology, v. 34, p. 233–236.

Gibson, T.G., Bybell, L.M., and Owens, J.P., 1993, Latest Paleocene lithologic and biotic events in neritic deposits of southwestern New Jersey: Paleoceanography, v. 8, p. 495–514.

Giusberti, L., Coccioni, R., Sprovieri, M., and Tateo, F., 2009, Perturbation at the sea floor during the Paleocene–Eocene thermal maximum: Evidence from benthic foraminifera at Contessa Road, Italy: Marine Micropaleontology, v. 70, p. 102–119.

Giusberti, L., Rio, D., Agnini, C., Backman, J., Fornaciari, E., Tateo, F., and Oddone, M., 2007, Mode and tempo of the Paleocene–Eocene thermal maximum in an expanded section from the Venetian pre-Alps: Geological Society of America Bulletin, v. 119, p. 391–412.

Gooday, A.J., 2003, Benthic foraminifera (Protista) as tools in deep-water paleoceanography: Environmental influences on faunal characteristics: Advances in Marine Biology, v. 46, p. 1–90.

John, C. M., Bohaty, S.M., Zachos, J.C., Sluijs, A., Gibbs, S., Brinkhuis, H., and Bralower, T.J., 2008, North American continental margin records of the Paleocene–Eocene thermal maximum: Implications for global carbon and hydrological cycling: Paleoceanography, v. 23, p. PA2217, doi: 10.1029/2007PA001465.

Jorissen, F.J., De Stigter, H.C., and Widmark, J.G.V., 1995, A conceptual model explaining benthic foraminiferal microhabitats: Marine Micropaleontology, v. 22, p. 3–15.

Jorissen, F.J., Fontanier, C., and Thomas, E., 2007, Paleoceanographical proxies based on deep-sea benthic foraminiferal assemblage characteristics, *in* Hillaire-Marcel, C., and de Vernal, A., eds., Proxies in Late Cenozoic Paleoceanography, pt. 2: Biological Tracers and Biomarkers: Elsevier. p. 263–326.

Kaiho, K., 1994, Benthic foraminiferal dissolved oxygen index and dissolved oxygen levels in the modern ocean: Geology, v. 22, p. 719–722.

Kaminski, M.A., and Gradstein, F., 2005, Atlas of Paleogene Cosmopolitan Deep-Water Agglutinated Foraminifera: Grzybowski Foundation Special Publication, v. 10, p. 1–548.

Kaminski, M.A., Kuhnt, W., and Radley, J. D., 1996, Paleocene–Eocene deep water agglutinated foraminifera from the Numidian Flysch (Rift, Northern Morocco): Their significance for the paleoceanography of the Gibraltar gateway: Journal of Micropaleontology, v. 15, p. 1–19.

Katz, M.E., Pak, D.K., Dickens, G.R., and Miller, K.G., 1999, The source and fate of massive carbon input during the latest Paleocene thermal maximum: Science, v. 286, p. 1531–1533.

Kelly, D.C., Bralower, T.J., and Zachos, J.C., 1998, Evolutionary consequences of the latest Paleocene thermal maximum for tropical planktonic foraminifera: Palaeogeography, Palaeoclimatology, Palaeoecology, v. 141, p. 139–161.

Kennett, J. P., and Stott, L. D., 1991, Abrupt deep-sea warming, palaeoceanographic changes and benthic extinctions at the end of the Palaeocene: Nature, v. 353, p. 225–229.

Koch, P.L., Zachos, J.C., and Gingerich, P.D., 1992, Correlation between isotope records near the Paleocene/Eocene boundary: Nature, v. 358, p. 319–322.

Koutsoukos, E.A.M., Mello, M.R., and Azambuja Filho, N.C., 1991, Micropalaeontological and geochemical evidence of mid-Cretaceous dysoxic-anoxic palaeoenvironments in the Sergipe Basin, northeastern Brazil, *in* Tyson, R.V., and Pearson, T.H., eds., Modern and Ancient Continental Shelf Anoxia: Geological Society Special Publications, London, v. 58, p. 427–447.

Kuhnt, W., and Kaminski, M.A., 1997, Cenomanian to lower Eocene deep-water agglutinated foraminifera from the Zumaya section, northern Spain: Annales Societatis Geologorum Poloniae, v. 67, p. 275–270.

Kuhnt, W., Kaminski, M.A., and Moullade, M., 1989, Late Cretaceous deep-water agglutinated foraminiferal assemblages from the North Atlantic and its marginal seas: Geologische Rundschau, v. 78, p. 1121–1140.

Kuhnt, W., Moullade, M., and Kaminski, M.A., 1996, Ecological structuring and evolution of deep sea agglutinated foraminifera—A review: Revue de Micropaléontologie, v. 39, p. 271–282.

Lourens, L.J., Sluijs, A., Kroon, D., Zachos, J.C., Thomas, E., Röhl, U., Bowles, J., and Raffi, I., 2005, Astronomical pacing of late Palaeocene to early Eocene global warming events: Nature, v. 435, p. 1083–1087.

Ly, A., and Kuhnt, W., 1994, Late Cretaceous benthic foraminiferal assemblages of the Casamanca Shelf (Senegal, NW Africa): Indication of a Late Cretaceous Oxygen Minimum Zone: Revue de Micropaléontologie, v. 37, p. 49–74.

Martins, V., Dubert, J., Jouanneau, J.M., Webber, O., Ferreira, E., Patinha, C., Alveirinho, J.M., and Rocha, F., 2007, A multiproxy approach of the Holocene evolution of shelf–slope circulation on the NW Iberian Continental Shelf: Marine Geology, v. 239, p. 1–18.

Molina, E., Arenillas, I., and Pardo, A., 1999, High resolution planktic foraminiferal biostratigraphy and correlation across the Paleocene/Eocene boundary in the Tethys: Bulletin de la Société Géologique de France, v. 170, p. 521–530.

Moore, E.A., and Kurtz, A.C., 2008, Black carbon in Paleocene-Eocene boundary sediments: A test of biomass combustion as the PETM trigger: Palaeogeography, Palaeoclimatology, Palaeoecology, v. 267, p. 147–152.

Murray, J.W., 1991, Ecology and Palaeoecology of Benthic Foraminifera: Longman Scientific and Technical, Harlow, Essex, UK, 397 p.

O'Brien, G.W., Milnes, A.R., Veeh, H.H., Heggie, D.T., Riggs, S.R., Cullen, D.J., Marshall, J.F., and Cook, P.J., 1990, Sedimentation dynamics and redox iron-cycling: Controlling factors for the apatite-glauconite association on the East Australian continental margin, *in* Notholt, A.J.G., and Jarvis, I., eds., Phosphorite Research and Development, *Geological Society Special Publications, London,* v. 52, p. 61–86.

Olsson, R.K., and Wise, S.W., 1987, Upper Paleocene to middle Eocene depositional sequences and hiatuses in the New Jersey Atlantic Margin, *in* Ross, C.A., and Haman, D., eds., Timing and Depositional History of Eustatic Sequences; Constraints of Seismic Stratigraphy: Cushman Foundation for Foraminiferal Research, Special Publications, v. 24, p. 99–112.

Ortiz, N., 1995, Differential patterns of benthic foraminiferal extinctions near the Paleocene/Eocene boundary in the North Atlantic and the western Tethys: Marine Micropaleontology, v. 26, p. 341–359.

Orue-Etxebarria, X., Apellaniz, E., Baceta, J.I., Coccioni, R., di Leo, R., Dinarés-Turrell, J., Galeotti, S., Monechi, S., Núñez-Betelu, K., Pares, J.M., Payros, A., Pujalte, V., Samso, J.M., Serra-Kiel, J., Schmitz, B., and Tosquella, J., 1996, Physical and biostratigraphic analysis of two prospective Paleocene-Eocene boundary stratotypes in the intermediate-deep water Basque Basin, western Pyrenees: The Trabakua Pass and Ermua sections: Neues Jahrbuch für Geologie und Paläontologie, Abhandlungen, v. 201, p. 179–242.

Orue-Etxebarria, X., Bernaola, G., Baceta, J.I., Angori, E., Caballero, F., Monechi, S., Pujalte, V., Dinarès-Turell, J., Apellaniz, E., and Payros, A, 2004, New constraints on the evolution of planktic foraminifera and calcareous nannofossils across the Paleocene-Eocene boundary interval: The Zumaia section revisited: Neues Jahrbuch für Geologie und Paläontologie, Abhandlungen, v. 234, p. 223–259.

Orue-Etxebarria, X., Pujalte, V., Bernaola, G., Apellaniz, E., Baceta, J.I., Payros, A., Núñez-Betelu, K., Serra-Kiel, J., and Tosquella, J., 2001, Did the Late Paleocene Thermal Maximum affect the evolution of larger foraminifers?: Evidences from calcareous plankton of the Campo section (Pyrenees, Spain): Marine Micropaleontology, v. 41, p. 45–71.

Pardo, A., Keller, G., and Oberhänsli, H., 1999, Paleoecologic and paleoceanographic evolution of the Tethyan Realm during the Paleocene–Eocene transition: Journal of Foraminiferal Research, v. 29, p. 37–57.

Pujalte, V., Baceta, J.I., Orue-Etxebarria, X., and Payros, A., 1998, Paleocene

strata of the Basque Country, western Pyrenees, northern Spain: Facies and sequence development in a deep-water starved basin, *in* Graciansky, P.C., Hardenbol, J., Jacquin, T., and Vail, P.R., eds., Mesozoic and Cenozoic Sequence Stratigraphy of European Basins: SEPM (Society for Sedimentary Geology) Special Publications, v. 60, p. 311–325.

Pujalte, V., Orue-Etxebarria, X., Schmitz, B., Tosquella, J., Baceta, J.I., Payros, A., Bernaola, G., Caballero, F., and Apellaniz, E., 2003, Basal Ilerdian (earliest Eocene) turnover of larger foraminifera: Age constraints based on calcareous plankton and δ13C isotopic profiles from new southern Pyrenean sections (Spain), *in* Wing, S., Gingerich, P., Schmitz, B., and Thomas, E., eds., Causes and Consequences of Globally Warm Climates in the Early Paleogene: Geological Society of America Special Paper no. 369, p. 205–221.

Röhl, U., Bralower, T.J., Norris, R.D., Wefer, G., 2000, New chronology for the late Paleocene thermal maximum and its environmental implications: Geology, v. 28, p. 927–930.

Röhl, U., Westerhold, T., Bralower, T.J., and Zachos, J.C., 2007, On the duration of the Paleocene–Eocene thermal maximum (PETM): Geochemistry, Geophysics, Geosystems, v. 8, Q12002, doi: 10.1029/2007GC001784.

Schmitz, B., Asaro, F., Molina, E., Monechi, S., Von Salis, K., and Speijer, R., 1997, High-resolution iridium, $\delta^{13}C$, $\delta^{18}O$, foraminifera and nannofossil profiles across the latest Paleocene benthic extinction event at Zumaya: Palaeogeography, Palaeoclimatology, Palaeoecology, v. 133, p. 49–68.

Schmitz, B., and Pujalte, V., 2007, Abrupt increase in seasonal extreme precipitation at the Paleocene-Eocene boundary: Geology, v. 35, p. 215–218.

Schmitz, B., Pujalte, V., and Núñez-Betelu, K., 2000, Climate and sea-level perturbations during the initial Eocene thermal maximum: Evidence from siliciclastic units in the Basque Basin (Ermua, Zumaia and Trabakua Pass), northern Spain: Palaeogeography, Palaeoclimatology, Palaeoecology, v. 165, p. 299–320.

Schönfeld, J., 2001, Benthic foraminifera and pore-water oxygen profiles: A reassessment of species boundary conditions at the Western Iberian Margin: Journal of Foraminiferal Research, v. 31, p. 86–107.

Sen Gupta, B.K., and Machain-Castillo, M.L., 1993, Benthic foraminifera in oxygen-poor habitats: Marine Micropaleontology, v. 20, p. 183–201.

Sliter, W.V., 1975, Foraminiferal life and residue assemblages from Cretaceous slope deposits: Geological Society of America Bulletin, v. 86, p. 897–906.

Sluijs, A., Bowen, G.J., Brinkhuis, H., Lourens, L.J., and Thomas, E., 2007a, The Palaeocene–Eocene Thermal maximum super greenhouse: Biotic and geochemical signatures, age models and mechanisms of climate change, *in* Williams, M., Haywood, A.M., Gregory, F.J., and Schmidt, D.N., eds., Deep Time Perspectives on Climate Change: Marrying the Signal from Computer Models and Biological Proxies: The Micropalaeontological Society, Special Publications, and Geological Society, London, p. 323–351.

Sluijs, A., Brinkhuis, H., Schouten, S., Bohaty, S.M., John, C.M., Zachos, J.C., Reichart, G.J., Sinninghe Damste, J., Crouch, E.M., and Dickens, G.R., 2007b, Environmental precursors to rapid light carbon injection at the Paleocene/Eocene boundary: Nature, v. 450, p. 1218–1221.

Speijer, R., and Wagner, T., 2002, Sea-level changes and black shales associated with the late Paleocene thermal maximum: Organic-geochemical and micropaleontologic evidence from the southern Tethyan margin (Egypt-Israel): Geological Society of America Special Paper, v. 356, p. 533–549.

Steineck, P.L., and Thomas, E., 1996, The latest Paleocene crisis in the deep sea: Ostracode succession at Maud Rise, Southern Ocean: Geology, v. 24, p. 583–586.

Stoll, H.M., 2005, Limited range of interspecific vital effects in coccolith stable isotopic records during the Paleocene–Eocene thermal maximum: Paleoceanography, v. 20, doi: 10.1029/2004PA001046.

Takeda, K., and Kaiho, K., 2007, Faunal turnovers in central Pacific benthic foraminifera during the Paleocene–Eocene thermal maximum: Palaeogeography, Palaeoclimatology, Palaeoecology, v. 251, p. 175–197.

Thomas, D.J., Bralower, T.J., and Zachos, J.C., 1999, New evidence for subtropical warming during the late Paleocene thermal maximum: Stable isotopes from Deep Sea Drilling Project 527, Walvis Ridge: Paleoceanography, v. 14, p. 561–570.

Thomas, D.J., Zachos, J.C., Bralower, T.J., Thomas, E., and Bohaty, S., 2002, Warming the fuel for fire: Evidence for the thermal dissociation of methane hydrate during the Paleocene–Eocene thermal maximum: Geology, v. 30, p. 1067–1070.

Thomas, E., 1989, Development of Cenozoic deep-sea benthic foraminiferal faunas in Antarctic waters, *in* Crame, J.A., eds., Origins and Evolution of the Antarctic Biota: Geological Society, London, Special Publications, v. 47, p. 283–296.

Thomas, E., 1990, Late Cretaceous through Neogene deep-sea benthic foraminifers (Maud Rise, Weddell Sea, Antarctica): Proceedings of the Ocean Drilling Program Scientific Results, v. 113, p. 571–594.

Thomas, E., 1998, The biogeography of the late Paleocene benthic foraminiferal extinction, *in* Aubry, M.P., Lucas, S., and Berggren, W.A., eds., Late Paleocene–Early Eocene Biotic and Climatic Events in the Marine and Terrestrial Records: Columbia University Press, New York, p. 214–243.

Thomas, E., 2003, Extinction and food at the seafloor: A high-resolution benthic foraminiferal record across the Initial Eocene Thermal Maximum, Southern Ocean Site 690, *in* Wing, S.L., Gingerich, P.D., Schmitz, B., and Thomas, E., eds., Causes and Consequences of Globally Warm Climates in the Early Paleogene: Geological Society of America Special Paper no. 369. Boulder, Colorado, p. 319–332.

Thomas, E., 2007, Cenozoic mass extinctions in the deep sea: What disturbs the largest habitat on Earth?, *in* Monechi, S., Coccioni, R., and Rampino, M., eds., Large Ecosystem Perturbations: Causes and Consequences: Geological Society of America Special Paper no. 424, p. 1–23.

Thomas, E., and Shackleton, N.J., 1996, The Paleocene–Eocene benthic foraminiferal extinction and stable isotope anomalies, *in* Knox, R.W., Corfield, R.M., and Dunay, R.E., eds., Correlation of the Early Paleogene in Northwest Europe. Geological Society, London, Special Publication, v. 101, p. 401–441.

Thomas, E., Zachos, J.C., and Bralower, T.J., 2000, Deep-sea environments on a warm Earth: Latest Paleocene–early Eocene, *in* Huber, B.T, MacLeod, K.G., and Wing, S.L., eds., Warm Climates in Earth History: Cambridge University Press, Cambridge, UK, p. 132–160.

Tjalsma, R.C., and Lohmann, G.P., 1983, Paleocene–Eocene bathyal and abyssal benthic foraminifera from the Atlantic Ocean: Micropaleontology, Special Publications, v. 4, p. 1–90.

Tremolada, F., and Bralower, T.J., 2004, Nannofossil assemblage fluctuations during the Paleocene–Eocene Thermal Maximum at Sites 213 (Indian Ocean) and 401 (North Atlantic Ocean): Palaeoceanographic implications: Marine Micropaleontology, v. 52, p. 107–116.

Van Morkhoven, F.P.C.M., Berggren, W.A., and Edwards, A.S., 1986, Cenozoic cosmopolitan deep-water benthic foraminifera: Bulletin des Centres de Recherches Exploration-Production Elf-Aquitaine, Memoir 11, Pau, France, p. 1–421.

Westerhold, T., Röhl, U., Laskar, J., Raffi, I., Bowles, J., Lourens, L.J., and Zachos, J.C., 2007, On the duration of magnetochrons C24r and C25n, and the timing of early Eocene global warming events: Implications from the ODP [Ocean Drilling Program] Leg 208 Walvis Ridge depth transect: Paleoceanography, v. 22, PA2201, doi: 10.1029/2006PA001322.

Wing, S.L., Harrington, G.J., Smith, F.A., Bloch, J.I., Boyer, D.M., and Freeman, K.H., 2005, Transient floral change and rapid global warming at the Paleocene-Eocene boundary: Science, v. 310, p. 993–996.

Zachos, J., Pagani, M., Sloan, L.C., Thomas, E., and Billups, K., 2001, Trends, rhythms, and aberrations in global climate 65 Ma to present: Science, v. 292, p. 686–693.

Zachos, J.C., Röhl, U., Schellenberg, S.A., Sluijs, A., Hodell, D.A., Kelly, D.C., Thomas, E., Nicolo, M., Raffi, I., Lourens, L.J., McCarren, H., and Kroon, D., 2005, Rapid acidification of the ocean during the Paleocene–Eocene Thermal Maximum: Science, v. 308, p. 1611–1615.

ACCEPTED DECEMBER 15, 2008